

# TSUNAMI HAZARD MAPS OF PORT ANGELES AND PORT TOWNSEND, WASHINGTON— MODEL RESULTS FROM A ~2,500- YEAR CASCADIA SUBDUCTION ZONE EARTHQUAKE SCENARIO

by Daniel W. Eungard, Corina Forson, Timothy J. Walsh,  
Frank I. González, Randall J. LeVeque,  
and Loyce M. Adams

WASHINGTON  
GEOLOGICAL SURVEY  
Map Series 2018-03  
August 2018

**[Partially superseded by Map Series 2022-01]**

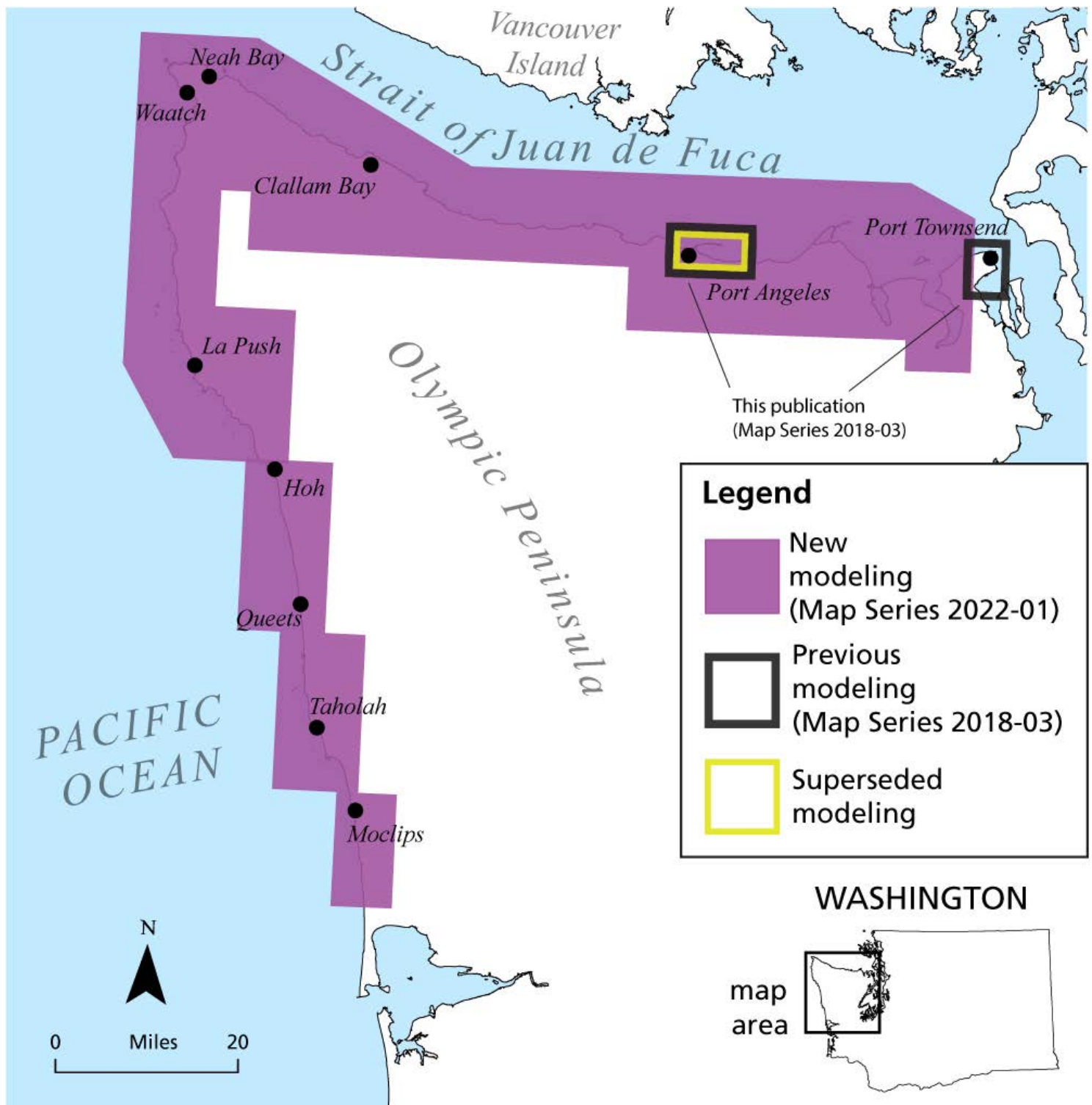
**INTERNALLY REVIEWED**



WASHINGTON STATE DEPARTMENT OF  
**NATURAL RESOURCES**  
WASHINGTON GEOLOGICAL SURVEY



# THIS PUBLICATION HAS BEEN PARTIALLY SUPERSEDED BY MAP SERIES 2022-01



Note that this publication has been partially superseded by Map Series 2022-01. The figure above shows which parts of this publication have been superseded (Map Sheets 1, 3, and 5 have been superseded, while Map Sheets 2, 4, and 6 have not been superseded). For those parts that have been superseded, please refer to Map Series 2022-01 for the most up-to-date tsunami inundation modeling.



# TSUNAMI HAZARD MAPS OF PORT ANGELES AND PORT TOWNSEND, WASHINGTON—MODEL RESULTS FROM A ~2,500-YEAR CASCADIA SUBDUCTION ZONE EARTHQUAKE SCENARIO

---

by Daniel W. Eungard, Corina Forson, Timothy J. Walsh,  
Frank I. González, Randall J. LeVeque,  
and Loyce M. Adams

WASHINGTON  
GEOLOGICAL SURVEY  
Map Series 2018-03  
August 2018

**[Partially superseded by Map Series 2022-01]**

*This publication has been subject to an iterative technical review process by at least one Survey geologist who is not an author.*

*This publication has also been subject to an iterative review process with Survey editors and cartographers and has been formatted by Survey staff.*



WASHINGTON STATE DEPARTMENT OF  
**NATURAL RESOURCES**  
WASHINGTON GEOLOGICAL SURVEY

## DISCLAIMER

Neither the State of Washington, nor any agency thereof, nor any of their employees, makes any warranty, express or implied, or assumes any legal liability or responsibility for the accuracy, completeness, or usefulness of any information, apparatus, product, or process disclosed, or represents that its use would not infringe privately owned rights. Reference herein to any specific commercial product, process, or service by trade name, trademark, manufacturer, or otherwise, does not necessarily constitute or imply its endorsement, recommendation, or favoring by the State of Washington or any agency thereof. The views and opinions of authors expressed herein do not necessarily state or reflect those of the State of Washington or any agency thereof.

This map product has been subjected to an iterative internal review process by agency geologists, cartographers, and editors and meets Map Series standards as defined by the Washington Geological Survey.

## INDEMNIFICATION

This item was funded by a National Tsunami Hazard Mitigation Program grant (award no. NA17NWS4670017) to the Washington Geological Survey from the Department of Commerce/National Oceanic and Atmospheric Administration. This does not constitute an endorsement by NOAA. Information about NTHMP is available at <http://nws.weather.gov/nthmp/>.

## WASHINGTON STATE DEPARTMENT OF NATURAL RESOURCES

Hilary S. Franz—*Commissioner of Public Lands*

## WASHINGTON GEOLOGICAL SURVEY

David K. Norman—*State Geologist*  
Timothy J. Walsh—*Assistant State Geologist*  
John P. Bromley—*Assistant State Geologist*

### Washington State Department of Natural Resources Washington Geological Survey

*Mailing Address:*  
MS 47007  
Olympia, WA 98504-7007

*Street Address:*  
Natural Resources Bldg, Rm 148  
1111 Washington St SE  
Olympia, WA 98501

*Phone:* 360-902-1450  
*Fax:* 360-902-1785  
*Email:* [geology@dnr.wa.gov](mailto:geology@dnr.wa.gov)  
*Website:* <http://www.dnr.wa.gov/geology>



*Publications and Maps:*  
[www.dnr.wa.gov/programs-and-services/geology/  
publications-and-data/publications-and-maps](http://www.dnr.wa.gov/programs-and-services/geology/publications-and-data/publications-and-maps)

*Washington Geology Library Searchable Catalog:*  
[www.dnr.wa.gov/programs-and-services/geology/  
washington-geology-library](http://www.dnr.wa.gov/programs-and-services/geology/washington-geology-library)

*Suggested Citation:* Eungard, D. W.; Forson, Corina; Walsh, T. J.; González, F. I.; LeVeque, R. J.; Adams, L. M., 2018, Tsunami hazard maps of Port Angeles and Port Townsend, Washington—Model results from a ~2,500-year Cascadia subduction zone earthquake scenario: Washington Geological Survey Map Series 2018-03, partially superseded by Map Series 2022-01, 6 sheets, scale 1:11,000 and 1:16,000, 11 p. text. [[http://www.dnr.wa.gov/publications/  
ger\\_ms2018-03\\_tsunami\\_hazard\\_pt\\_angeles\\_pt\\_townsend.zip](http://www.dnr.wa.gov/publications/ger_ms2018-03_tsunami_hazard_pt_angeles_pt_townsend.zip)]



Daniel W Eungard

*Daniel W. Eungard*  
August 2018

# Contents

Introduction .....	1
Cascadia Subduction Zone .....	3
Recurrence Intervals .....	3
Earthquake Magnitudes and Slip Distributions .....	5
AD 1700 Earthquake .....	5
Pre-AD 1700 Earthquakes .....	6
Modeling Approach and Results .....	7
Inundation .....	7
Current Speed.....	7
Timing of Tsunami and Initial Water Disturbance.....	8
Limitations of the Model.....	9
Acknowledgments.....	9
References.....	10

## FIGURES

Figure 1. Location map of the Port Angeles and Port Townsend study area.....	2
Figure 2. Photo of tsunami deposits at Discovery Bay, WA.....	3
Figure 3. Map of southwest Oregon showing tsunami deposits and abrupt subsidence locations .....	4
Figure 4. Schematic view of the confluence test for extensive seismic shaking.....	5
Figure 5. L1 splay fault model diagram and map of vertical ground deformation during an L1 scenario Cascadia earthquake.....	6
Figure 6. Map of initial ground and seafloor deformation from the L1 scenario near Port Angeles and Port Townsend.....	6
Figure 7. Modeled tsunami wave variations over time for simulated tide gauges near Port Angeles and Port Townsend.....	8
Figure 8. Schematic diagram of chronologic events following a CSZ earthquake and tsunami.....	9

## TABLES

Table 1. Published tsunami hazard maps for Washington .....	2
Table 2. Estimates of earthquake recurrence on the Cascadia subduction zone.....	5

## MAP SHEET

Map Sheet 1. Tsunami inundation of Port Angeles
Map Sheet 2. Tsunami inundation of Port Townsend
Map Sheet 3. Tsunami current velocity of Port Angeles
Map Sheet 4. Tsunami current velocity of Port Townsend
Map Sheet 5. Detailed tsunami inundation of Port Angeles
Map Sheet 6. Detailed tsunami inundation of Port Townsend





---

# Tsunami Hazard Maps of Port Angeles and Port Townsend, Washington—Model Results from a ~2,500-year Cascadia Subduction Zone Earthquake Scenario

by Daniel W. Eungard<sup>1</sup>, Corina Forson<sup>1</sup>, Timothy J. Walsh<sup>1</sup>, Frank I. González<sup>2</sup>, Randall J. LeVeque<sup>3</sup>, and Loyce M. Adams<sup>3</sup>

<sup>1</sup> Washington Geological Survey  
MS 47007  
Olympia, WA 98504-7007

<sup>2</sup> Department of Earth and Space Sciences  
University of Washington  
Johnson Hall 070  
Box 351310  
Seattle, WA 98195-1310

<sup>3</sup> Department of Applied Mathematics  
University of Washington  
Lewis Hall 201  
Box 353925  
Seattle, WA 98195-3925

## ABSTRACT

New tsunami modeling along the Strait of Juan de Fuca within an area surrounding the communities of Port Angeles and Port Townsend uses a simulated magnitude 9 earthquake event along the Cascadia subduction zone (L1 scenario) with a maximum slip of ~89 ft (27 m), inferred to be a ~2,500 year event. This new Cascadia subduction zone earthquake scenario aims to approximate the seismic design requirements in the building code standard for critical facilities, and the tsunami modeling is more conservative (greater inundation) than previous models. Modeling results indicate that sea level immediately following the earthquake gradually recedes to a maximum drawdown of ~6.5 ft (2 m) before the first tsunami wave arrival. This first wave is projected to inundate as high as 21 ft (6.4 m) locally in Port Angeles and Port Townsend approximately 60 minutes and 100 minutes respectively following the earthquake. Current velocities from the tsunami waves locally approach 26 knots, presenting a significant navigational hazard to the maritime community. Tsunami wave inundation is expected to continue over 8 hours and remain hazardous to maritime operations for more than 24 hours. This study is limited in that modeling does not account for tide stage, tidal currents, liquefaction, or minor topographic changes that would locally modify the effects of tsunami waves. Due to these limitations, this modeling should not be used for site-specific tsunami inundation assessment or for determining effects on the built environment. However, this model is an appropriate tool for evacuation and recovery planning.

## INTRODUCTION

In 1995, Congress directed the National Oceanic and Atmospheric Administration (NOAA) to develop a plan to protect the west coast from tsunamis generated by the nearby Cascadia subduction zone (CSZ). A panel of representatives from NOAA, the Federal Emergency Management Agency (FEMA), the U.S. Geological Survey (USGS) and the five Pacific coast states wrote and submitted the plan to Congress, which created the National Tsunami Hazard Mitigation Program (NTHMP) in 1996. The NTHMP is designed to reduce the impact of tsunamis through warning guidance, hazard assessment, education, and mitigation.

A key component of the hazard assessment for tsunamis is delineation of areas subject to tsunami inundation, and is the first step in developing evacuation products. Because local tsunami waves may reach nearby coastal communities within 60 to 90 minutes after the earthquake, there will be limited time to issue formal warnings.

Map Sheets 1 through 6 depict modeled tsunami inundation and current velocity for the Strait of Juan de Fuca in

the communities of Port Angeles and Port Townsend from a CSZ earthquake (Fig. 1); they are part of a series of tsunami inundation maps produced by the Washington Geological Survey, in cooperation with the Washington Emergency Management Division, as a contribution to the NTHMP (Table 1). These maps are produced using computer models of earthquake-generated tsunamis from the CSZ developed by the Department of Applied Mathematics, University of Washington.

Previous inundation modeling for this area (Walsh and others, 2002a and 2002b) was for simulated events on the CSZ designated 1A and 1A with asperity (Myers and others, 1999; Priest and others, 1997). For several years, this modeling was the only source of tsunami hazard information for emergency managers and local communities.

Recent studies (Witter and others, 2011) have inferred: (1) variability in both the amount of slip and slip distribution from the paleo-tsunami record; and (2) their L1 scenario on the CSZ is a more conservative choice, that is, it is less likely to

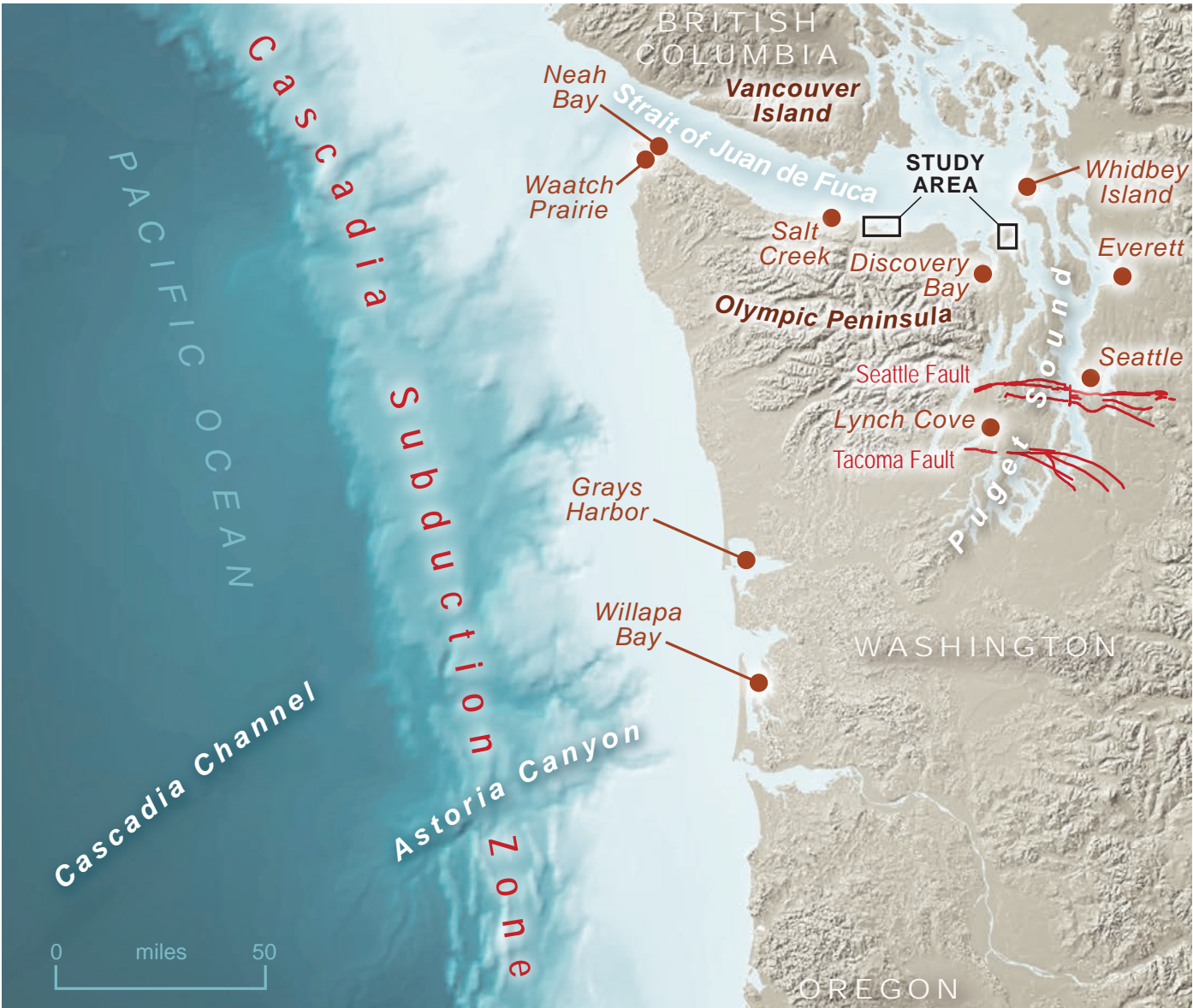


**Figure 1.** Location map of the Port Angeles and Port Townsend study area, Cascadia subduction zone, major offshore channels, and major crustal faults known to produce tsunamis.

**Table 1.** Published tsunami hazard maps for Washington. CSZ, Cascadia subduction zone. \*1A with asperity model incorporates localized area of offshore uplift.

Location	Reference	Modeled Scenario
Anacortes–Bellingham	Eungard and others (2018a)	CSZ L1
Southwest Washington	Eungard and others (2018b)	CSZ L1
San Juan Islands	Walsh and others (2016)	CSZ L1
Everett	Walsh and others (2014)	Seattle Fault
Tacoma	Walsh and others (2009)	Tacoma and Seattle faults
Anacortes–Whidbey Island	Walsh and others (2005)	CSZ 1A and 1A with asperity*
Bellingham	Walsh and others (2004)	CSZ 1A and 1A with asperity*
Neah Bay	Walsh and others (2003a)	CSZ 1A and 1A with asperity*
Quileute area	Walsh and others (2003b)	CSZ 1A and 1A with asperity*
Seattle	Walsh and others (2003c)	Seattle Fault
Port Angeles	Walsh and others (2002a)	CSZ 1A and 1A with asperity*
Port Townsend	Walsh and others (2002b)	CSZ 1A and 1A with asperity*
southern Washington coast	Walsh and others (2000)	CSZ 1A and 1A with asperity*



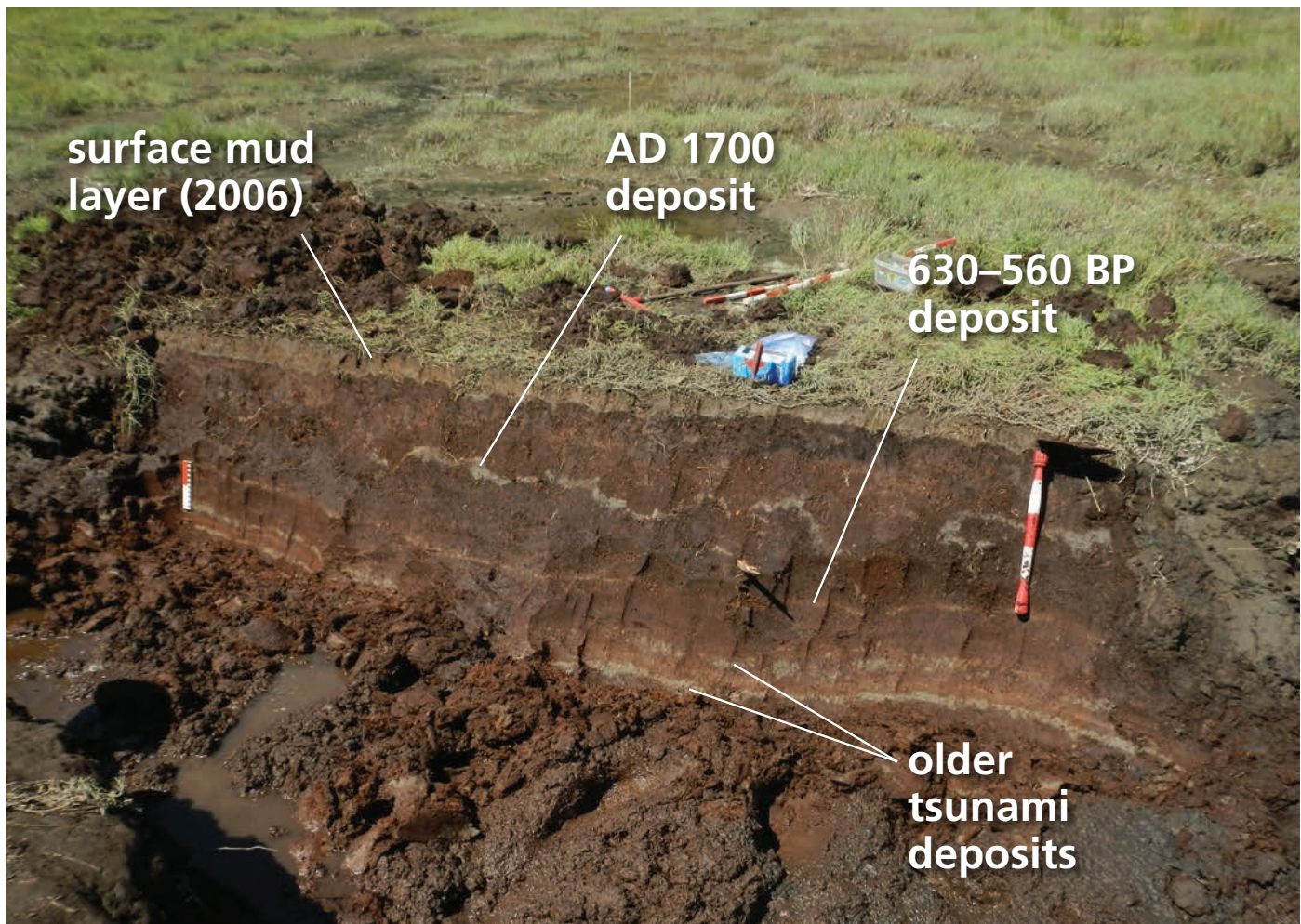


**Figure 2.** Photo of tsunami deposits (sand layers bounded by silty clays) at Discovery Bay, WA. Four tsunami deposits visible in photo include inferred AD 1700 sand layer that was later disturbed by marsh restoration projects, a sand layer dated at 630 to 560 radiocarbon years BP (Garrison-Laney and Miller, 2017), and two older sand layers beneath. The topmost mud layer was deposited in 2006, following marsh restoration. Photo by Carrie Garrison-Laney (Washington Sea Grant).

be exceeded than scenario 1A. This modeled scenario (L1) is a close approximation to design requirements for critical facilities in the Washington State building code for seismic hazards. The scenario represents the most probable of the maximum considered CSZ earthquake that a facility may be subjected to during its operational lifetime. (See *Earthquake Magnitudes and Slip Distributions* for more information on model scenarios.)

## CASCADIA SUBDUCTION ZONE

Research over the last few decades about the occurrence of great earthquakes off the British Columbia, Washington, Oregon, and northern California coastlines (Atwater, 1992; Atwater and others, 1995) has led to concern that locally generated tsunamis will leave little time for response. Numerous workers found geologic evidence of tsunami deposits attributed to the CSZ in at least 59 localities from northern California to southern Vancouver Island (Peters and others, 2003). While most of these locations are on the outer coast, inferred CSZ tsunami deposits were identified along the Strait of Juan de Fuca at Salt Creek (Hutchinson and others, 2013), as far east as Discovery Bay (near Port Townsend)(Fig. 2; Williams and others, 2005), on the west

shore of Whidbey Island (Fig. 1; Williams and Hutchison, 2000), and as far south as Lynch Cove at the terminus of Hood Canal (Garrison-Laney, 2017). Heaton and Snavely (1985) reported that Makah Tribe stories may record a tsunami washing through Waatch Prairie near Cape Flattery (Fig. 1). Ludwin (2002) has found additional stories from native peoples up and down the coast that appear to corroborate this and include apparent references to associated strong ground shaking.

Additionally, high-resolution dendrochronology (Jacoby and others, 1997; Yamaguchi and others, 1997) from locations in Washington indicates that the timing of the last CSZ earthquake correlates with historical records of a distant-source tsunami in Japan (Satake and others, 1996) on January 26, AD 1700.

## Recurrence Intervals

Estimates of the frequency of CSZ earthquakes are derived from several lines of evidence: coastal submergence events, paleo-tsunami deposits (Fig. 2), and offshore turbidite deposits. Great subduction zone earthquakes commonly cause coseismic subsidence (Plafker, 1969; Plafker and Savage, 1970). Where this subsidence occurs in coastal marshes, marsh deposits may be abruptly overlain by estuarine mud, indicating sudden



submergence and drowning of upland surfaces (Atwater, 1992). Atwater and Hemphill-Haley (1997) reported six sudden submergence events in Willapa Bay over the last 3,500 years (Table 2). Their data imply an average recurrence interval of about 500 to 540 years, but individual intervals vary between 100 and 1,300 years.

Researchers working in Oregon have found a somewhat different record farther south. Using marsh stratigraphy and inferred tsunami deposits, Kelsey and others (2002) found a 5,500-year record of 11 earthquake events at Sixes River in southern Oregon (Fig. 3). These records included an abrupt subsidence event not observed on the southern Washington coast. Kelsey and others (2005) examined Bradley Lake on the southern Oregon coast near Bandon and found that it recorded inferred tsunami deposits with an average recurrence interval of ~390 years. This discrepancy implies that some tsunamis generated by earthquakes on the CSZ did not produce abrupt subsidence in southern Washington. A possible explanation is that the earthquake did not rupture the entire length of the subduction zone, resulting in a spatially heterogeneous response in the geologic record. Nelson and others (2006) examined the degree of overlap and amount of abrupt subsidence at eight

sites along the Oregon and Washington coasts and concluded that rupture lengths (and therefore earthquake magnitudes) varied—ruptures along the northern CSZ are generally long, whereas ruptures along the southern CSZ are more variable in both length and recurrence interval.

Another approach to inferring recurrence intervals is the correlation of turbidites—deposits of sediment gravity flows, or turbidity currents—at the base of the continental shelf. Adams (1990) inferred that turbidite deposits in Cascadia Channel and Astoria Canyon (Fig. 4) were triggered by great earthquakes. If turbidity currents are triggered independently, at different times, and at multiple submarine canyon heads that merge with a main channel, then their deposits should be additive in the main channel. For example, if a channel has three tributaries, each of which has ten independent turbidites, there would be 30 turbidites in the main channel. However, if the turbidites are triggered simultaneously—which would likely be the case if they were initiated by a great earthquake—they should coalesce. In this case, the maximum number of turbidites in the main channel would be no more than the maximum number found in any individual channel. Oregon State University researchers logged 13 turbidites in both Cascadia Channel and Astoria

Canyon, from multiple deep-sea cores that were stratigraphically above the Mazama ash (radiocarbon dated at about 6,845 radiocarbon years BP [calibrated to about 7,700 cal yr BP])(Adams, 1990). These findings suggest that 13 CSZ ruptures occurred since the Mazama ash was deposited. Adams (1990) therefore inferred an average recurrence interval of  $590 \pm 170$  years.

Goldfinger and others (2012) tested Adams' (1990) hypothesis by collecting numerous additional cores in the sea floor along the Cascadia continental margin. Their effort greatly expands the geographic and chronologic range of observation, and increases observation density. Goldfinger and others (2012) inferred from their record of turbidite deposits that the CSZ is segmented, with full-length ruptures having a recurrence interval similar to those estimated by Adams (1990) and Atwater and Hemphill-Haley (1997), but with additional partial-length ruptures offshore Oregon and northern California.

Combining full-length and partial ruptures on the CSZ, Goldfinger and others (2012) estimated a recurrence interval of ~240 years for earthquakes off Oregon and northern California, but still 500 to 530 years offshore Washington and British Columbia.



**Figure 3.** Map of southwest Oregon showing tsunami deposits and abrupt subsidence locations used by Kelsey and others (2002, 2005) to determine CSZ earthquake recurrence intervals.

**Table 2.** Estimates of earthquake recurrence on the Cascadia subduction zone. - - - indicates no data.

Events over time interval	Average recurrence interval in years; range if given	Section of CSZ	References	Major evidence
6 submergence events in 3,500 years	500–540 average, 100–300 to 1,300	northern	Atwater and Hemphill-Haley (1997)	submergence events
11 submergence events in 5,500 years	510	southern	Kelsey and others (2002)	marsh stratigraphy and tsunami deposits
13 tsunamis, 17 disturbances in 7,000 years	- - -	southern	Kelsey and others (2005)	marine incursions and disturbance events in Bradley Lake
- - -	variable	whole	Nelson and others (2006)	multiple
- - -	590 ± 170	northern	Adams (1990)	turbidites in Astoria Canyon and Cascadia Channel
19 or 20 full-margin turbidites in 10,000 years; 22 turbidites restricted to the south	500–530 average for full-margin rupture; ~240 full-margin plus southern only	whole and partial	Goldfinger and others (2012)	turbidites along Cascadia margin
20 full-margin turbidites in 10,000 years; 3 turbidites on a segment running from northern California to Juan de Fuca Channel; 1 turbidite off Washington and B.C. only	500–530 average for full-margin rupture; ~434 full-margin plus shorter ruptures adjacent to Washington	whole and partial	Goldfinger and others (2017)	turbidites along Cascadia margin

1 **River** delivers sediment to the sea.

2 **Sediment** settles on the continental shelf.

3 **An earthquake** shakes the continental shelf and slope.

4 **Shaken sediment** descends submarine canyons as turbidity currents.

5 **Turbidity currents** merge where tributaries meet. Resulting deposits are visible in sediment cores.

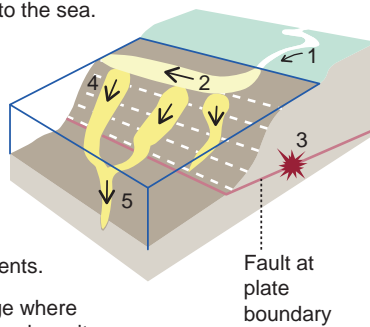


**Figure 4.** Schematic view of the confluence test for extensive seismic shaking, first used as a guide to fault rupture length by Adams (1990). Adams assumed that extensive shaking enables turbidity currents to descend different submarine channels at the same time and merge below channel confluences. Atwater and others (2014) dispute the reliability of this indicator.

Earthquakes that rupture only the northern part of the CSZ are also a possibility. Goldfinger and others (2017) revised this chronology slightly, extending several ruptures farther north to include Washington and inferring an additional event offshore Washington and southern British Columbia only. In Discovery Bay and in the northeast of the Olympic Peninsula, Williams and others (2005) observed nine muddy sand beds bearing marine diatoms that interrupt a 2,500-year-old sequence of peat deposits beneath a tidal marsh. If all of these are tsunami deposits, then it is likely that some of them record events that are either not full-length ruptures of the CSZ or come from some other source. The ages of four of these beds, refined by Garrison-Laney and Miller (2017), overlap with known late-Holocene tsunamis generated by full-length ruptures of the CSZ. Diatom assemblages in peat deposits bracketing these four beds do not indicate a concurrent change in elevation at Discovery Bay. This suggests that coseismic subsidence has been negligible as far east as Discovery Bay. However, one inferred tsunami deposit

is accompanied by several decimeters of abrupt subsidence, which is interpreted as the result of deformation associated with an upper plate fault (Williams and others, 2005). Other sand sheets in the sequence may represent tsunamis generated by partial ruptures of the CSZ, by upper plate fault earthquakes, or by landslides (Garrison-Laney and Miller, 2017), none of which triggered turbidity currents. This implies that either some CSZ earthquakes do not leave turbidite deposits in Cascadia Channel, or that some tsunami deposits were generated by other events such as local earthquakes or landslides. Atwater and others (2014) also questioned whether the absence of turbidites along the northern CSZ necessarily proves the absence of ground shaking, or rather is influenced by differences in sediment supply and in the differences in flow paths down tributary channels. They also questioned some of the correlations among widely spaced sites—used to infer the length of fault rupture—that were used by Goldfinger and others (2012).

## Earthquake Magnitudes and Slip Distributions

### AD 1700 EARTHQUAKE

It is believed that the last earthquake on the Cascadia subduction zone was about magnitude (Mw) 9.0 (Satake and others, 1996; 2003). Satake and others (2003) tested various rupture lengths, slip amounts, and observed tsunami wave heights in Japan for the AD 1700 event. They estimated that this event had a rupture length of 684 mi (~1,100 km) and 62 ft (19 m) of coseismic slip on an offshore, full-slip zone with linearly decreasing slip on a down-dip partial-slip zone, suggesting a magnitude of 8.7 to 9.2. They inferred that the most likely magnitude was 9.0 based on the correlation between estimates of coseismic subsidence from paleo-seismic studies and the subsidence predicted by their scenario dislocation models.

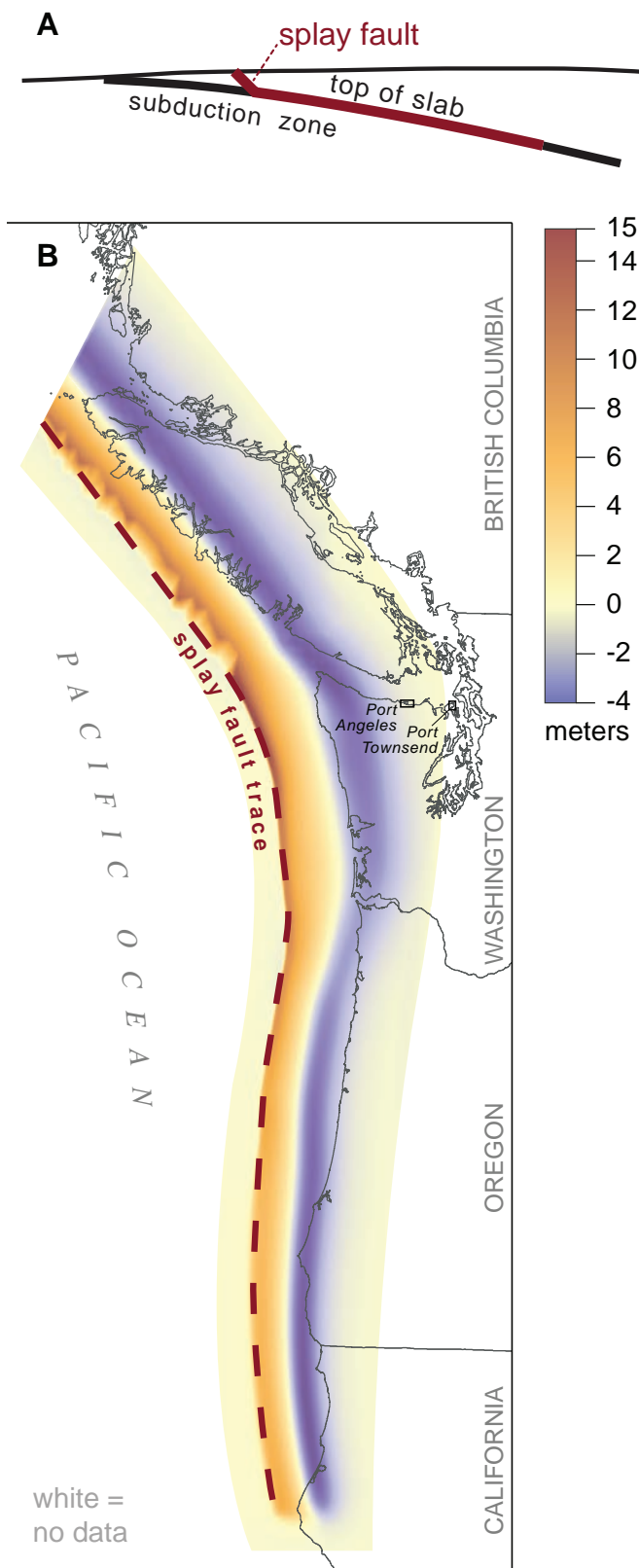


**Figure 5.** L1 splay fault model diagram (A) and map of vertical ground deformation (B) during a great Cascadia earthquake in the L1 scenario of Witter and others (2011), modified by Edison Gica and Diego Arcas (PMEL, personal commun., 2018) to extend farther northwest beyond Witter and others' (2011) original truncation line.

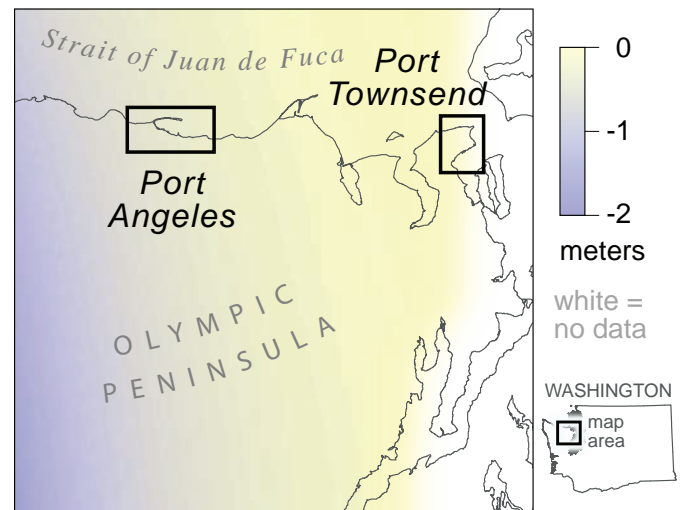


**Figure 6.** Map of initial ground and seafloor deformation from the L1 scenario for Port Angeles and Port Townsend. Deformation for the Port Townsend area is negligible.

## PRE-AD 1700 EARTHQUAKES

### Partial-Length Rupture Models

The magnitudes and slip distributions of earlier CSZ earthquakes are less well constrained. Inferences of shorter ruptures that affect only the southern part of the CSZ generally imply smaller magnitude earthquakes. Tsunamis from several postulated shorter ruptures limited to the southern part of the CSZ were modeled by Priest and others (2014), who concluded that the tsunamis they generated were significantly smaller in Washington than those generated by full-length ruptures. A partial CSZ rupture restricted to the north was suggested by Goldfinger and others (2013) and Peterson and others (2013). This northern rupture was later confirmed by Goldfinger and others (2017), but paleo-seismic data for it is insufficient to generate a tsunami model. These smaller events are not considered further here.

### Full-Length Rupture Models

Witter and others (2012) combined: (1) turbidite data from Goldfinger and others (2012); (2) correlation of inferred tsunami deposits with turbidites in Bradley Lake; and (3) inferred tsunami deposits in the Coquille River estuary at Bandon, Oregon that extend as much as 6.2 mi (10 km) farther inland than the AD 1700 tsunami deposits (Witter and others, 2003). They inferred from this that tsunamis generated by Cascadia over the last 10,000 years had been highly variable, with some larger than the one in AD 1700. They constructed 15 scenarios of full-length ruptures defining vertical seafloor deformation used to simulate tsunami inundation at Bandon, Oregon. Rupture models include slip partitioned to a splay fault in the accretionary wedge and models that vary the up-dip limit of slip on a buried megathrust fault. Slip estimates were made from several sources. Total turbidite volume was estimated from the thickness averaged over all the paleo-seismic records, which Goldfinger and others (2012) correlated to earthquake magnitude. This was combined with estimates of the convergence rate for different segments of the subduction zone multiplied by the time since the previous event to estimate total accumulated strain since the previous event (Witter and others, 2012). Witter and others (2011, 2012) performed



numerical tsunami simulations at Bradley Lake and Bandon, Oregon, and then compared them using a logic tree that ranked model consistency with geophysical and geological data from the distribution of inferred tsunami deposits. They found that the deposits were broadly compatible with their larger scenarios.

Witter and others (2011) concluded that scenario L1—a splay fault model with a maximum slip of 88.6 ft (27 m) and an average slip of 42.6 ft (13 m)—produced a tsunami that equaled or exceeded 95 percent of the variability in their simulations (Fig. 5). Other ‘L’ earthquake scenarios (L2 and L3) have the same amount of slip but somewhat different distributions across the strike of the subduction zone. In other words, the L1 scenario produces tsunamis as big as, or bigger than most other models. Witter and others (2011) also estimated the size of the earthquakes that generated turbidites along the full length of the CSZ. They concluded that three earthquakes in the last ~10,000 years were probably similar to scenario L and only one was larger (table 1 in Witter and others, 2011). The inter-event times between pairs of inferred L earthquakes are ~1,800 and ~4,600 years. Another way to estimate recurrence frequency is that if three earthquakes in the last 10,000 years are of size L, then these types of events have an average recurrence interval between 2,500 and 5,000 years. If this truly represents 95 percent of the hazard over a 10,000-year period, then scenario L earthquakes have a long recurrence interval and likely are of a similar probability of occurrence as the International Building Code seismic standard of 2 percent probability of exceedance in 50 years. Colloquially, this scenario is known as a ~2,500-year event.

NOAA Pacific Marine Environmental Laboratory (PMEL) modified the original ground deformation model of Witter and others (2011) to test whether faulting to the north of the L1 truncation line would have a significant impact on tsunami inundation along the Strait of Juan de Fuca and inner waters of Washington State. This modification (Edison Gica and Diego Arcas, PMEL, personal commun., 2018) uses a smooth extension of slip distributed to the northwest following the approximate strike of the CSZ along the coast of British Columbia. Tsunami modeling results show that the additional ground deformation from this modification contributes little change to tsunami waves entering the Strait of Juan de Fuca.

## MODELING APPROACH AND RESULTS

This tsunami inundation model is based on a numerical model of waves generated by a L1 CSZ scenario earthquake as described in Witter and others (2011) as adapted in Walsh and others (2016), and modified by Edison Gica and Diego Arcas (personal commun., 2018). The numerical model, produced by the Geoclaw portion of the Clawpack software (Clawpack Development Team, 2017; Mandli and others, 2016; LeVeque and others, 2011), uses a finite-volume method of solving shallow wave equations (Berger and others, 2011). The model utilizes an adaptive-mesh-grid of topographic and bathymetric elevations and calculates wave elevation and velocity for each cell at specified time intervals to simulate the generation, propagation, and inundation of a tsunami following a L1 scenario CSZ earthquake. The model is calculated for mean high water and does not include tidal effects.

The L1 scenario is a splay-fault model in which all slip is partitioned into a thrust fault in the accretionary wedge that has an approximate 30° landward dip and the same sense of movement as the megathrust; this results in a much higher, narrower area of uplift than a fault rupture on the megathrust, which dips landward much more shallowly and reaches farther seaward than the splay fault. The land surface along the Strait of Juan de Fuca is modeled to subside slightly during ground shaking (Fig. 6) with decreasing subsidence eastward from the subduction zone. Port Angeles is modeled to subside by 1.6 ft (0.5 m), and eastward, subsidence becomes negligible near Port Townsend. This is consistent with paleo-seismic investigations which suggest approximately 0.5 m or less of coseismic subsidence at Salt Creek (Hutchinson and others, 2013) and little or no subsidence at Discovery Bay (Williams and others, 2005; Garrison-Laney, 2017).

Compared to previous modeling efforts (Walsh and others, 2002a, 2002b) the newer L1 modeling study area does not extend as far beyond the Port Angeles and Port Townsend downtown core, but is at a higher resolution and incorporates higher quality elevation data from lidar and multibeam bathymetry where available.

## Inundation

Inundation depth bins on Map Sheets 1 and 2 were selected based on their implications for life safety. These bins are defined as: (1) less than knee high (0–2.5 ft; 0–0.75 m); (2) knee to head high (2.5–6 ft; 0.75–1.8 m); and (3) above head height (>6 ft; >1.8 m). These depths approximate the hazard posed to a person if caught within the tsunami zone. At 0 to 2.5 ft inundation, survival is likely if steps are taken to avoid the direct force of a wave, such as entering a building, or standing on the leeward side of an obstacle (tree or power pole). From 2.5 to 6 ft inundation, survival is unlikely if caught in the open; however, climbing onto the roof of a single-story structure or entering a structure more than one story tall may improve survivability. At >6 ft inundation, survival is highly unlikely if caught either out in the open or within or on most conventional structures. Survival remains highly likely within or on a reinforced and specially designed building, such as a vertical evacuation structure. Modeled inundation is also shown using the full range of values on Map Sheets 5 and 6.

Tsunami inundation from this scenario is expected to cover most of the low-lying areas below the coastal bluffs in both Port Angeles and Port Townsend. Inundation depths may reach ~21 ft (6.4 m) along the shoreline, with significant inundation modeled in the downtown core and harbor areas of both communities in addition to the entirety of Ediz Hook in Port Angeles. Inundation would be expected to continue along the coastal bluffs and up river channels beyond the study area boundaries at both Port Angeles and Port Townsend (Walsh and others 2002a, 2002b).

## Current Speed

The modeled current speed (Map Sheets 3 and 4) is shown in four ranges (0–3 knots, 3–6 knots, 6–9 knots, and >9 knots) following the port damage categorization of Lynett and others (2014). These ranges approximate hazard to ships and docking facilities, representing no expected damage, minor/moderate damage

possible, major damage possible, and extreme damage possible, respectively. Modeled current speeds locally approach 26 knots with the highest velocities expected near the shore where the tsunami–tide interactions are likely to be most significant. Certain topographic features produce strong currents with potential for the formation of vortices; examples of these are located at Ediz Hook, Point Wilson, and Point Hudson.

## Timing of Tsunami and Initial Water Disturbance

Wave arrival times are estimated from the moment the earthquake begins to the moment the water first rises above high tide (mean high water). For the arrival times shown on Map Sheets 5 and 6, this is not the timing of maximum inundation. Several minutes may pass between first wave arrival and maximum inundation. Strong earthquake shaking may persist for as many as five minutes in this scenario, reducing the available time to evacuate to less than indicated. Figure 7 shows a series of simulated tide-gauge records in the near-shore Port Angeles and

Port Townsend study areas. At Port Angeles (Fig. 7, paper mill, USCG station, and ferry terminal) the approximate timing of the initial water disturbance is a gradual fall in sea level from a leading wave trough beginning at 8 minutes and reaching -6.5 ft (2 m) at 40 minutes. This is followed by a rapidly rising wave commencing at 60 minutes and reaching a peak of ~20 ft (6.1 m) at 80 minutes. Port Townsend also has a gradual drop in sea level reaching 6.5 ft (2 m) 90 minutes after the earthquake, rapidly rising to ~21 ft (6.4 m) at 120 minutes. Figure 8, a conceptual visualization, demonstrates this sequence of events. There may be some locations where the first wave may not be the highest (Fig. 7, Point Wilson), where later waves may create a greater amount of inundation. Waves <5 ft (1.5 m) are expected for 12 hours following the earthquake. Minor inundation and strong currents posing a hazard to rescue and recovery operations may continue for at least 24 hours after the earthquake. For comparison, the January 26, AD 1700 earthquake along the CSZ produced a tsunami that may have lasted as many as 20 hours in Japan (Satake and others, 2003; Atwater and others, 2005).

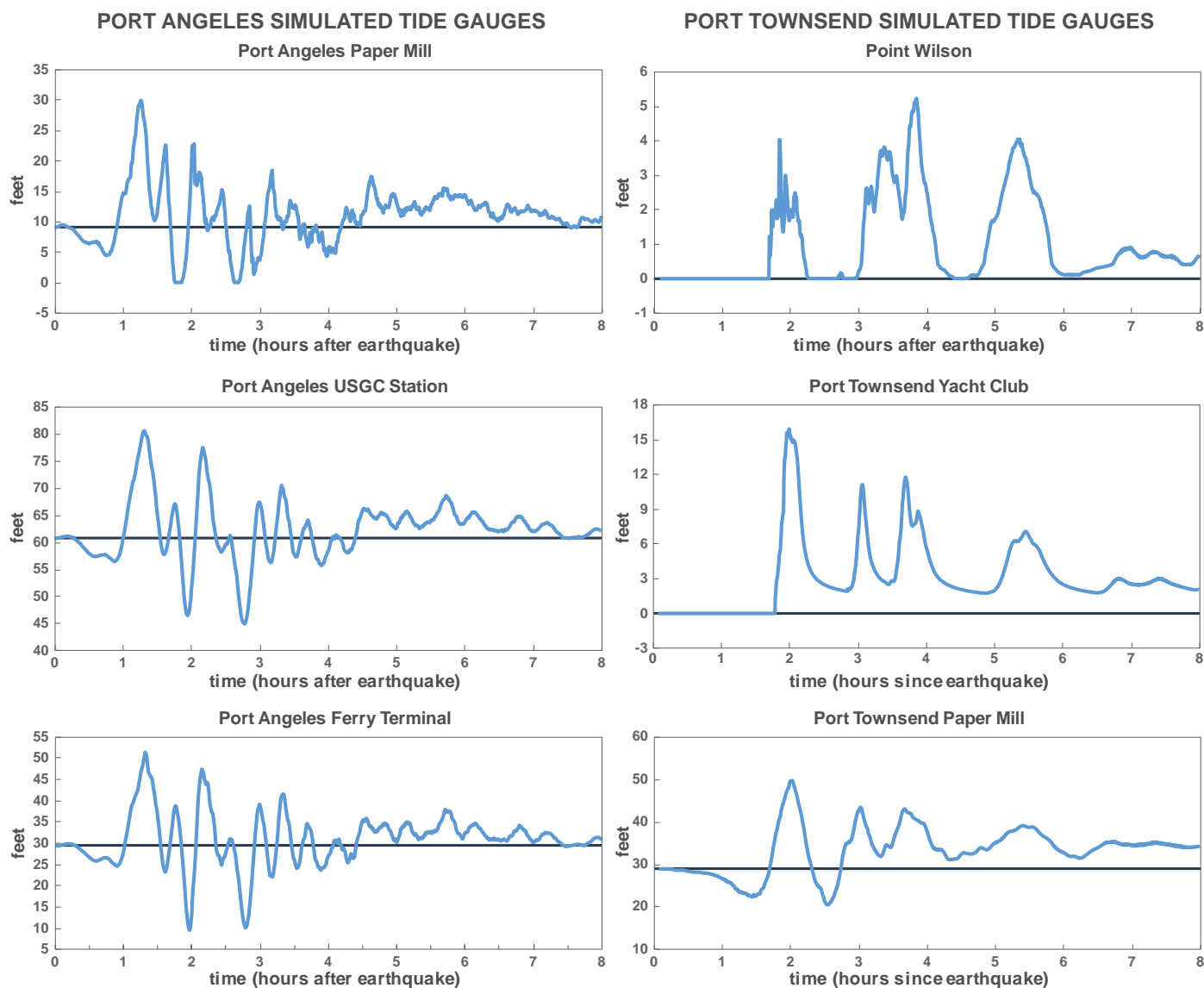


**Figure 7.** Modeled tsunami wave variations over time (light blue lines) for simulated tide gauges near Port Angeles (left column) and Port Townsend (right column). Dark blue horizontal lines indicate static mean high water elevation at simulated tide gauges. See Map Sheets 1 and 2 for locations.



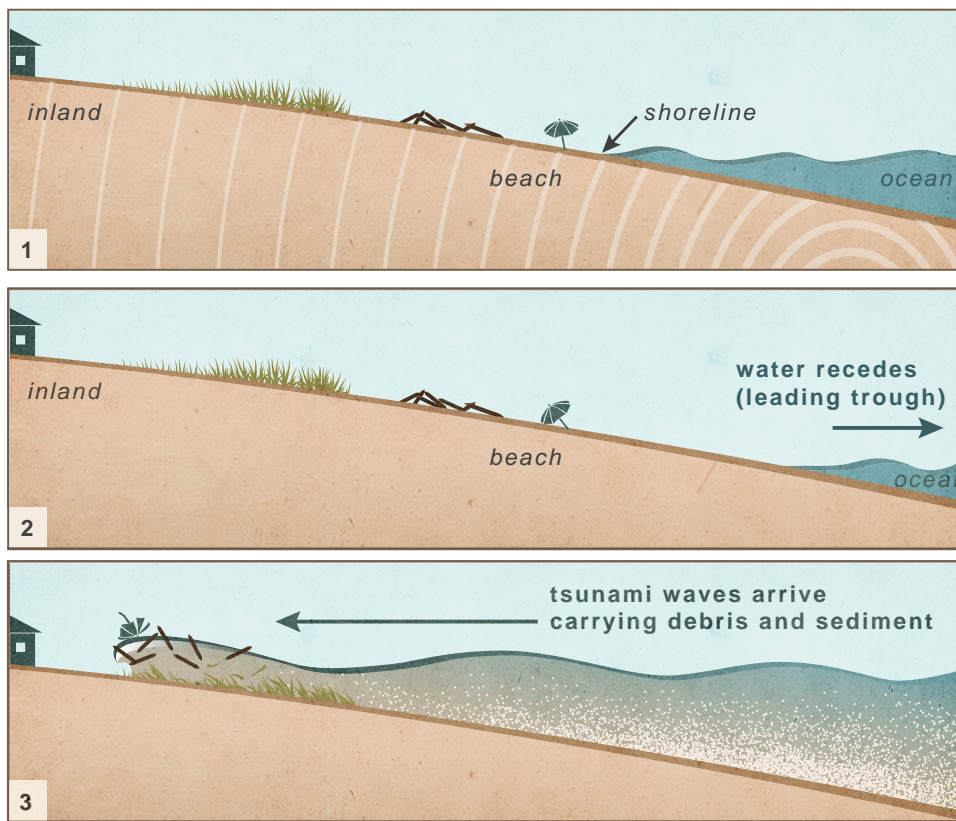


**Figure 8.** Schematic diagram of chronologic events following a CSZ earthquake and tsunami: (1) Earthquake on the CSZ produces strong shaking that will last several minutes; (2) The first indication of an incoming tsunami wave to the Port Angeles and Port Townsend region will be a gradual drop in water level prior to arrival of the first tsunami wave; and (3) Tsunami waves begin to arrive ~60 min (at Port Angeles) to ~100 min (at Port Townsend) following the earthquake. These powerful waves carry sediment and debris onshore and to higher elevations. The inundation continues for at least 8 hours, locally posing a hazard to search, rescue, and recovery efforts.

The March 27, 1964, Mw9.2 earthquake near Anchorage, Alaska produced a wave in Washington that peaked at least 12 hours after the first arrival (Walsh and others, 2000).

## LIMITATIONS OF THE MODEL

Because the characteristics of the tsunami depend on the initial seafloor deformation of the earthquake, which is poorly understood, the largest source of uncertainty is the input earthquake. The earthquake scenario used in this model was selected to approximate the 2 percent probability of exceedance in 50 years (~2,500-year event), but the next earthquake may have a more complex slip distribution than the simplified scenario we used and thus the ensuing tsunami may differ. Witter and others (2011) suggest that the most likely full-length CSZ earthquake will have an average slip of about two-thirds of the L1 scenario and therefore generate a smaller tsunami than modeled here.

These model results do not include potential tsunamis from coseismic landslides or ruptures on nearby crustal faults. This modeling does not incorporate localized topographic changes caused by liquefaction, such as settlement or sand blows. Liquefaction is a site-specific issue and is inappropriate at this map scale. The model does not include the influences of changes in tides and is referred to mean high water. The tide stage can amplify or reduce the impact of a tsunami on a specific community. For example, the diurnal range (the difference in height between mean higher high water and mean lower low water) is 2.27 ft (0.69 m) and 2.84 ft (0.87 m) at the Port Angeles (<https://tidesandcurrents.noaa.gov/stationhome.html?id=9444090>) and Port Townsend (<https://tidesandcurrents.noaa.gov/stationhome.html?id=9444900>) tide gauges respectively. The model also does

not include interaction with tidal currents, which can be additive, or if in opposite directions, can steepen the tsunami wave front and cause a breaking wave.

The resolution of the modeling is also limited by the bathymetric and topographic data used to make the elevation grid. The elevation grid was created with a variety of data sources, with grid cells ranging from ~3 ft (1 m) for the topographic grid and 16 to 3,937 ft (5–1,200 m) for the bathymetric grid. Coarse grids do not capture small topographic features that can influence the tsunami locally. This generally leads to greater modeled inundation than would be produced by finer grids, except in narrow or constricted channels or along steep topographic features.

Small, isolated gaps in inundation exist (for example, at the Port Angeles port log yard). Additionally, transient features (log piles, aggregate piles, etc.), misclassified buildings or treetops, and some actual high areas may not survive the impact of tsunami waves. The maps retain these gaps in inundation to remain true to the model results. However, it is highly likely that these small areas will be inundated during a tsunami.

While modeling can be a useful tool to guide evacuation planning, model uncertainties and insufficient spatial resolution make this modeling unsuitable for site-specific tsunami mitigation planning.

## ACKNOWLEDGMENTS

This project was supported by the National Tsunami Hazards Mitigation Program (NTHMP) in cooperation with Clallam and Jefferson Counties, and the Washington Emergency Management Division.

## REFERENCES

- Adams, John, 1990, Paleoseismicity of the Cascadia subduction zone—Evidence from turbidites off the Oregon–Washington margin: *Tectonics*, v. 9, no. 4, p. 569-583.
- Atwater, B. F., 1987, Evidence for great Holocene earthquakes along the outer coast of Washington State: *Science*, v. 236, no. 4804, p. 942-944.
- Atwater, B. F., 1992, Geologic evidence for earthquakes during the past 2,000 years along the Copalis River, southern coastal Washington: *Journal of Geophysical Research*, v. 97, no. B2, p. 1901-1919.
- Atwater, B. F.; Nelson, A. R.; Clague, J. J.; Carver, G. A.; Yamaguchi, D. K.; Bobrowsky, P. T.; Bourgeois, Joanne; Darienzo, M. E.; Grant, W. C.; Hemphill-Haley, Eileen; Kelsey, H. M.; Jacoby, G. C.; Nishenko, S. P.; Palmer, S. P.; Peterson, C. D.; Reinhart, M. A., 1995, Summary of coastal geologic evidence for past great earthquakes at the Cascadia subduction zone: *Earthquake Spectra*, v. 11, no. 1, p. 1-18.
- Atwater, B. F.; Hemphill-Haley, Eileen, 1997, Recurrence intervals for great earthquakes of the past 3,500 years at northeastern Willapa Bay, Washington: U.S. Geological Survey Professional Paper 1576, 108 p. [<https://pubs.er.usgs.gov/publication/pp1576>]
- Atwater, B. F.; Musumi-Rokkaku, Satoko; Satake, Kenji; Tsuji, Yoshinobu; Ueda, Kazue; Yamaguchi, D. K., 2005, The orphan tsunami of 1700—Japanese clues to a parent earthquake in North America: University of Washington Press and U.S. Geological Survey Professional Paper 1707, 133 p. [[https://pubs.usgs.gov/pp/pp1707/pp1707\\_front.pdf](https://pubs.usgs.gov/pp/pp1707/pp1707_front.pdf)]
- Atwater, B. F.; Carson, R. C.; Griggs, G. B.; Johnson, H. P.; Salmi, M. S., 2014, Rethinking turbidite paleoseismology along the Cascadia subduction zone: *Geology*, v. 42, no. 9, p. 827-830.
- Berger, M. J.; George, D. L.; LeVeque R. J.; and Mandli, K. M., 2011, The GeoClaw software for depth-averaged flows with adaptive refinement: *Advances in Water Resources*, v. 34, pp. 1195-1206.
- Clawpack Development Team, 2017, Clawpack Version 5.4.0 [<http://www.clawpack.org>, doi:10.5281/zenodo.262111]
- Eungard, D. W.; Forson, Corina; Walsh, T. J.; Gica, Edison; Arcas, Diego, 2018b, Tsunami hazard maps of southwest Washington—Model results from a ~2,500-year Cascadia subduction zone earthquake scenario: Washington Geological Survey Map Series 2018-01, originally published March 2018, 6 sheets, scale 1:48,000, 11 p. text. [[http://www.dnr.wa.gov/publications/ger\\_ms2018-01\\_tsunami\\_hazard\\_southwest\\_washington.zip](http://www.dnr.wa.gov/publications/ger_ms2018-01_tsunami_hazard_southwest_washington.zip)]
- Eungard, D. W.; Forson, Corina; Walsh, T. J.; Gica, Edison; Arcas, Diego, 2018a, Tsunami hazard maps of the Anacortes–Bellingham area, Washington—Model results from a ~2,500-year Cascadia subduction zone earthquake scenario: Washington Geological Survey Map Series 2018-02, 6 sheets, scale 1:30,000, 10 p. text. [[http://www.dnr.wa.gov/publications/ger\\_ms2018-02\\_tsunami\\_hazard\\_anacortes\\_bellingham.zip](http://www.dnr.wa.gov/publications/ger_ms2018-02_tsunami_hazard_anacortes_bellingham.zip)]
- Garrison-Laney, C. E., 2017, Tsunamis and sea levels of the past millennium in Puget Sound, Washington: University of Washington Doctor of Philosophy thesis, 166 p.
- Garrison-Laney, C. E.; Miller, I., 2017, Tsunamis in the Salish Sea: Recurrence, sources, hazards, *In* Haugerud, R. A.; Kelsey, H. M., 2017, From the Puget Lowland to east of the Cascade Range—Geologic excursions in the Pacific Northwest: Geological Society of America Field Trip Guide v. 49, p. 67-78.
- Goldfinger, Chris; Nelson, C. H.; Morey, A. E.; Johnson, J. E.; Patton, J. R.; Karabanov, Eugene; Gutierrez-Pastor, Julia; Eriksson, A. T.; Gracia, Eulalia; Dunhill, Gita; Enkin, R. J.; Dallimore, Audrey; Vallier, Tracy, 2012, Turbidite event history—Methods and implications for Holocene paleoseismicity of the Cascadia subduction zone: U.S. Geological Survey Professional Paper 1661-F, 170 p., 64 figures. [<https://pubs.usgs.gov/pp/pp1661f/>]
- Goldfinger, C.; Morey, A. E.; Black, B.; Beeson, J.; Nelson, C. H.; Patton, J., 2013, Spatially limited mud turbidites on the Cascadia margin: segmented earthquake ruptures?: *Natural Hazards and Earth System Sciences*, v. 13, no. 8, p. 2109-2146.
- Goldfinger, C.; Galer, S.; Beeson, J.; Hamilton, T.; Black, B.; Romsos, C.; Patton, J.; Nelson, C. H.; Hausmann, R.; Morey, A., 2017, The importance of site selection, sediment supply, and hydrodynamics—A case study of submarine paleoseismology on the northern Cascadia margin, Washington USA: *Marine Geology*, v. 384.
- Heaton, T. H.; Snavely, P. D., Jr., 1985, Possible tsunami along the northwestern coast of the United States inferred from Indian traditions: *Seismological Society of America Bulletin*, v. 75, no. 5, p. 1455-1460.
- Hutchinson, Ian; Peterson, C. D.; Sterling, S. L., 2013, Late Holocene tsunami deposits at Salt Creek, Washington, USA: *Science of Tsunami Hazards*, v. 32, p. 221-235.
- Jacoby, G. C.; Bunker, D. E.; Benson, B. E., 1997, Tree-ring evidence for an A.D. 1700 Cascadia earthquake in Washington and northern Oregon: *Geology*, v. 25, no. 11, p. 999-1002.
- Kelsey, H. M.; Nelson, A. R.; Hemphill-Haley, Eileen; Witter, R. C., 2005, Tsunami history of an Oregon coastal lake reveals a 4,600 yr record of great earthquakes on the Cascadia subduction zone: *Geological Society of America*, v. 117, no. 7-8, p. 1009-1032.
- Kelsey, H. M.; Witter, R. C.; Hemphill-Haley, Eileen, 2002, Plateboundary earthquakes and tsunamis of the past 5,500 yr, Sixes River estuary, southern Oregon: *Geological Society of America Bulletin*, v. 114, no. 3, p. 298-314.
- LeVeque, R. J.; George, D. L.; Berger, M. J., 2011, Tsunami modeling with adaptively refined finite volume methods: *Acta Numerica*, v. 20, p. 211-289.
- Ludwin, R. S., 2002, Cascadia megathrust earthquakes in Pacific Northwest Indian myths and legends: *TsuInfo Alert*, v. 4, no. 2, p. 6-10. [[https://www.dnr.wa.gov/publications/ger\\_tsuinfo\\_2002\\_v4\\_no2.pdf](https://www.dnr.wa.gov/publications/ger_tsuinfo_2002_v4_no2.pdf)]
- Lynett, P. J.; Borrero, Jose; Son, Sangyoung; Wilson, Rick; Miller, Kevin, 2014, Assessment of the tsunami-induced current hazard: *Geophysical Research Letters*, v. 41, iss. 6, p. 2048-2055.
- Mandli, K. T.; Ahmadi, A. J.; Berger, M.; Calhoun, D.; George, D. L.; Hadjimichael, Y.; Ketcheson, D. I.; Lemoine, G. I.; LeVeque, R. J., 2016, Clawpack: building an open source ecosystem for solving hyperbolic PDEs. *PeerJ Computer Science*, 2:e68.
- Myers, E. P., III; Baptista, A. M.; Priest, G. R., 1999, Finite element modeling of potential Cascadia subduction zone tsunamis: *Science of Tsunami Hazards*, v. 17, no. 1, p. 3-18.
- Nelson, A. R.; Kelsey, H. M.; Witter, R. C., 2006, Great earthquakes of variable magnitude at the Cascadia subduction zone: *Quaternary Research*, v. 65, no. 3, p. 354-365.
- Peters, Robert; Jaffé, B. E.; Gelfenbaum, Guy; Peterson, C. D., 2003, Cascadia tsunami deposit database: U.S. Geological Survey Open-File Report 03-13, 25 p. [accessed May 6, 2004 at <http://geopubs.wr.usgs.gov/open-file/of03-13/>]
- Peterson, C. D.; Cruikshank, K. M.; Darienzo, M. E.; Wessen, G. C.; Butler, V. L.; Sterling, S. L., 2013, Cosismic subsidence and paleotsunami run-up records from latest Holocene deposits in the Waatch Valley, Neah Bay, northwest Washington, U.S.A.—Links to great earthquakes in the northern Cascadia margin: *Journal of Coastal Research*, v. 29, no. 1, p. 157-172.
- Plafker, George, 1969, Tectonics of the March 27, 1964, Alaska earthquake: U.S. Geological Survey Professional Paper 543-1, 74 p., 2 sheets, scales 1:2,000,000 and 1:500,000. [<https://pubs.usgs.gov/pp/0543i/>].
- Plafker, George; Savage, J. C., 1970, Mechanism of the Chilean earthquakes of May 21 and 22, 1960: *Geological Society of America Bulletin*, v. 81, no. 4, p. 1001-1030.



- Priest, G. R.; Myers, E. P., III; Baptista, A. M.; Fleuck, Paul; Wang, Kelin; Kamphaus, R. A.; Peterson, C. D., 1997, Cascadia subduction zone tsunamis—Hazard mapping at Yaquina Bay, Oregon: Oregon Department of Geology and Mineral Industries Open-File Report O-97-34, 144 p. [<http://www.oregongeology.org/pubs/ofr/O-97-34.pdf>]
- Priest, G. R.; Zhang, Yinglong; Witter, R. C.; Wang, Kelin; Goldfinger, Chris; Stimely, Laura, 2014, Tsunami impact to Washington and northern Oregon from segment ruptures on the southern Cascadia subduction zone: *Natural Hazards*, v. 72, no. 2, p. 849-870.
- Satake, Kenji; Shimazaki, Kunihiro; Tsuji, Yoshinobu; Ueda, Kazuo, 1996, Time and size of a giant earthquake in Cascadia inferred from Japanese tsunami records of January 1700: *Nature*, v. 379, no. 6562, p. 246-249.
- Satake, Kenji; Wang, Kelin; Atwater, B. F., 2003, Fault slip and seismic moment of the 1700 Cascadia earthquake inferred from Japanese tsunami description: *Journal of Geophysical Research*, v. 108, no. B11, 2535.
- Walsh, T. J.; Caruthers, C. G.; Heintz, A. C.; Myers, E. P., III; Baptista, A. M.; Erdakos, G. B.; Kamphaus, R. A., 2000, Tsunami hazard map of the southern Washington coast—Modeled tsunami inundation from a Cascadia subduction zone earthquake: Washington Division of Geology and Earth Resources Geologic Map GM-49, 1 sheet, scale 1:100,000, with 12 p. text. [[http://www.dnr.wa.gov/publications/ger\\_gm49\\_tsunami\\_hazard\\_southern\\_coast.zip](http://www.dnr.wa.gov/publications/ger_gm49_tsunami_hazard_southern_coast.zip)]
- Walsh, T. J.; Myers, E. P., III; Baptista, A. M., 2002a, Tsunami inundation map of the Port Angeles, Washington area: Washington Division of Geology and Earth Resources Open File Report 2002-1, 1 sheet, scale 1:24,000. [[http://www.dnr.wa.gov/publications/ger\\_ofr2002-1\\_tsunami\\_hazard\\_portangeles.pdf](http://www.dnr.wa.gov/publications/ger_ofr2002-1_tsunami_hazard_portangeles.pdf)]
- Walsh, T. J.; Myers, E. P., III; Baptista, A. M., 2002b, Tsunami inundation map of the Port Townsend, Washington area: Washington Division of Geology and Earth Resources Open File Report 2002-2, 1 sheet, scale 1:24,000. [[http://www.dnr.wa.gov/publications/ger\\_ofr2002-2\\_tsunami\\_hazard\\_porttownsend.pdf](http://www.dnr.wa.gov/publications/ger_ofr2002-2_tsunami_hazard_porttownsend.pdf)]
- Walsh, T. J.; Myers, E. P., III; Baptista, A. M., 2003a, Tsunami inundation map of the Neah Bay, Washington, area: Washington Division of Geology and Earth Resources Open File Report 2003-2, 1 sheet, scale 1:24,000. [[http://www.dnr.wa.gov/publications/ger\\_ofr2003-2\\_tsunami\\_hazard\\_neahbay.pdf](http://www.dnr.wa.gov/publications/ger_ofr2003-2_tsunami_hazard_neahbay.pdf)]
- Walsh, T. J.; Myers, E. P., III; Baptista, A. M., 2003b, Tsunami inundation map of the Quileute, Washington, area: Washington Division of Geology and Earth Resources Open File Report 2003-1, 1 sheet, scale 1:24,000. [[http://www.dnr.wa.gov/publications/ger\\_ofr2003-1\\_tsunami\\_hazard\\_quileute.pdf](http://www.dnr.wa.gov/publications/ger_ofr2003-1_tsunami_hazard_quileute.pdf)]
- Walsh, T. J.; Titov, V. V.; Venturato, A. J.; Mofjeld, H. O.; González, F. I., 2003c, Tsunami hazard map of the Elliott Bay area, Seattle, Washington—Modeled tsunami inundation from a Seattle Fault earthquake: Washington Division of Geology and Earth Resources Open File Report 2003-14, 1 sheet, scale 1:50,000. [[http://www.dnr.wa.gov/publications/ger\\_ofr2003-14\\_tsunami\\_hazard\\_elliottbay.pdf](http://www.dnr.wa.gov/publications/ger_ofr2003-14_tsunami_hazard_elliottbay.pdf)]
- Walsh, T. J.; Titov, V. V.; Venturato, A. J.; Mofjeld, H. O.; González, F. I., 2004, Tsunami hazard map of the Bellingham area, Washington—Modeled tsunami inundation from a Cascadia subduction zone earthquake: Washington Division of Geology and Earth Resources Open File Report 2004-15, 1 sheet, scale 1:50,000. [[http://www.dnr.wa.gov/publications/ger\\_ofr2004-15\\_tsunami\\_hazard\\_bellingham.pdf](http://www.dnr.wa.gov/publications/ger_ofr2004-15_tsunami_hazard_bellingham.pdf)]
- Walsh, T. J.; Titov, V. V.; Venturato, A. J.; Mofjeld, H. O.; González, F. I., 2005, Tsunami hazard map of the Anacortes-Whidbey Island area, Washington—Modeled tsunami inundation from a Cascadia subduction zone earthquake: Washington Division of Geology and Earth Resources Open File Report 2005-1, 1 sheet, scale 1:62,500. [[http://www.dnr.wa.gov/publications/ger\\_ofr2005-1\\_tsunami\\_hazard\\_anacortes\\_whidbey.pdf](http://www.dnr.wa.gov/publications/ger_ofr2005-1_tsunami_hazard_anacortes_whidbey.pdf)]
- Walsh, T. J.; Arcas, Diego; Venturato, A. J.; Titov, V. V.; Mofjeld, H. O.; Chamberlin, C. C.; González, F. I., 2009, Tsunami hazard map of Tacoma, Washington—Model results for Seattle fault and Tacoma fault earthquake tsunamis: Washington Division of Geology and Earth Resources Open File Report 2009-9, 1 sheet, scale 1:24,000. [[http://www.dnr.wa.gov/publications/ger\\_ofr2009-9\\_tsunami\\_hazard\\_tacoma.pdf](http://www.dnr.wa.gov/publications/ger_ofr2009-9_tsunami_hazard_tacoma.pdf)]
- Walsh, T. J.; Arcas, Diego; Titov, V. V.; Chamberlin, C. C., 2014, Tsunami hazard map of Everett, Washington: Model results for magnitude 7.3 and 6.7 Seattle fault earthquakes: Washington Division of Geology and Earth Resources Open File Report 2014-03, 1 plate, scale 1:32,000. [[http://www.dnr.wa.gov/publications/ger\\_ofr2014-03\\_tsunami\\_hazard\\_everett.pdf](http://www.dnr.wa.gov/publications/ger_ofr2014-03_tsunami_hazard_everett.pdf)]
- Walsh, T. J.; Gica, Edison; Arcas, Diego; Titov, V. V.; Eungard, D. W., 2016, Tsunami hazard maps of the San Juan Islands, Washington—Model results from a Cascadia subduction zone earthquake scenario: Washington Division of Geology and Earth Resources Map Series 2016-01, 4 sheets, scale 1:24,000 and 1:48,000, 9 p. text. [[http://www.dnr.wa.gov/publications/ger\\_ms2016-01\\_tsunami\\_hazard\\_san\\_juan\\_islands.zip](http://www.dnr.wa.gov/publications/ger_ms2016-01_tsunami_hazard_san_juan_islands.zip)]
- Williams, H. F. L.; Hutchinson, Ian, 2000, Stratigraphic and microfossil evidence for late Holocene tsunamis at Swantown Marsh, Whidbey Island, Washington: *Quaternary Research*, v. 54, no. 2, p. 218-227.
- Williams, H. F. L.; Hutchinson, Ian; Nelson, A. R., 2005, Multiple sources for late-Holocene tsunamis at Discovery Bay, Washington State, USA: *The Holocene*, v. 15, no. 1, p. 60-73.
- Witter, R. C.; Kelsey, H. M.; and Hemphill-Haley, E., 2003, Great Cascadia earthquakes and tsunamis of the past 6,700 years, Coquille River estuary, southern coastal Oregon: *Geological Society of America Bulletin*, v. 115, no. 10, p. 1289-1306.
- Witter, R. C.; Zhang, Yinglong; Wang, Kelin; Priest, G. R.; Goldfinger, Chris; Stimely, L. L.; English, J.T.; Ferro, P. A., 2011, Simulating tsunami inundation at Bandon, Coos County, Oregon, using hypothetical Cascadia and Alaska earthquake scenarios: Oregon Department of Geology and Mineral Industries Special Paper 43, 57 p. [<http://www.oregongeology.org/pubs/sp/p-SP-43.html>]
- Witter, R. C.; Zhang, Yinglong; Wang, Kelin; Goldfinger, Chris; Priest, G. R.; Allan, J. C., 2012, Coseismic slip on the southern Cascadia megathrust implied by tsunami deposits in an Oregon lake and earthquake-triggered marine turbidites: *Journal of Geophysical Research*, v. 117, no. B10303, 17 p.
- Yamaguchi, D. K.; Atwater, B. F.; Bunker, D. E.; Benson, B. E.; Reid, M. S., 1997, Tree-ring dating the 1700 Cascadia earthquake: *Nature*, v. 389, p. 922-923.